IEEE Photonics Journal
An IEEE Photonics Society Publication

Open Access

Fluence as a Function of Weight: A Photobiomodulation Therapy (PBMT) Spinal Cord Injury (SCI) Rat Model—A Computational Study

Volume 12, Number 6, December 2020

Ali Shuaib
Ali K. Bourisly
Eman Alazmi

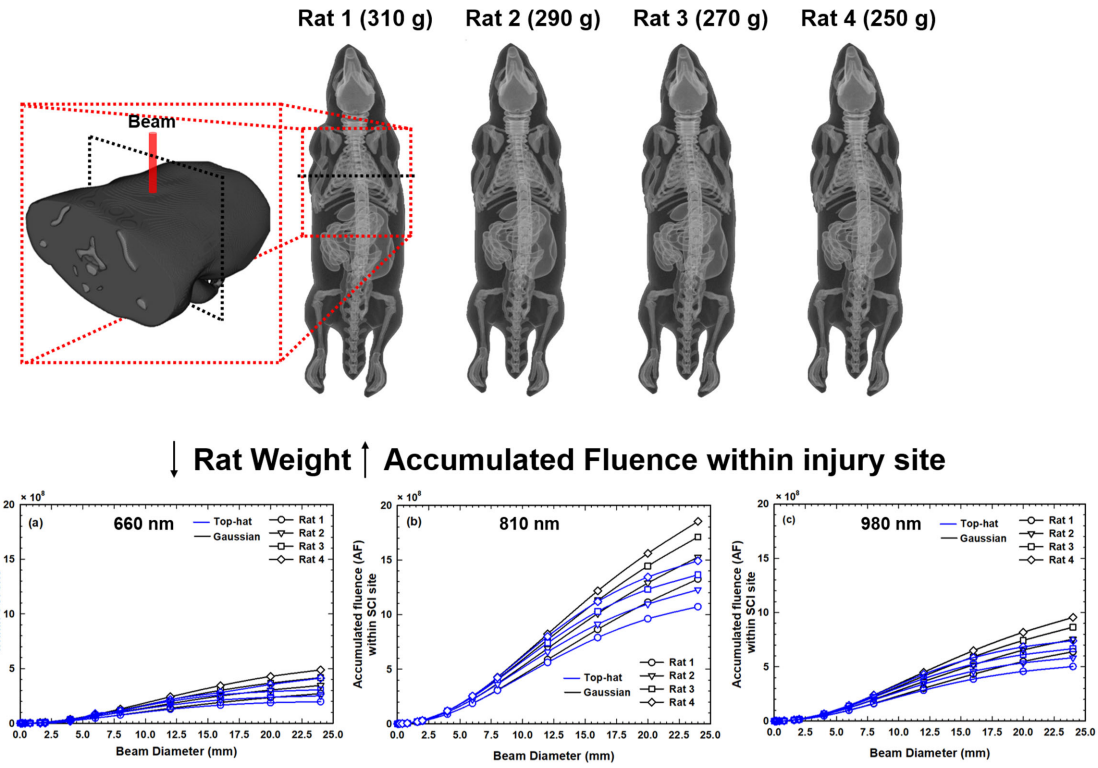

DOI: 10.1109/JPHOT.2020.3033476

Fluence as a Function of Weight: A Photobiomodulation Therapy (PBMT) Spinal Cord Injury (SCI) Rat Model—A Computational Study

Ali Shuaib ,[1] Ali K. Bourisly,[1] and Eman Alazmi[2]

[1]Biomedical Engineering Unit, Department of Physiology, Faculty of Medicine, Kuwait University, Safat 13110, Kuwait
[2]Department of Physics, Faculty of Science, Kuwait University, Safat 13060, Kuwait

DOI:10.1109/JPHOT.2020.3033476

Manuscript received September 10, 2020; accepted October 20, 2020. Date of publication October 23, 2020; date of current version November 12, 2020. Corresponding author: Ali Shuaib (e-mail: ali.shuaib@ku.edu.kw).

Abstract: A spinal cord injury (SCI) is caused by damage to neurons in the spinal cord, which interrupts neural signal conduction via axonal tracts, causing either total or partial paralysis. Researchers have proven that photobiomodulation therapy (PBMT) can affect nerve repair, causing enhanced functionality. Many PBMT studies have examined contusion SCIs in rats by employing a fixed fluence applied to the skin over the course of the treatment without considering the animal weight, which could affect the fluence delivered to the SCI site. This study performed Monte Carlo simulations using four computer-simulated rat models, all 11 weeks of age but each one having a different weight, and used various irradiation parameters to assess the impact of these factors on the fluence delivery at the SCI site. When the weight of the rat decreased, the fluence delivered to the SCI site increased. The findings also demonstrated that the greatest percentage rise in the fluence delivered to the SCI site occurred when employing a 660 nm Gaussian beam. The rat weight and irradiation parameters had a significant effect on the fluence delivered to the SCI site in rats. Thus, when assessing the effectiveness of PBMT, researchers must consider how much fluence reaches the injury site rather than how much fluence is applied to the skin.

Index Terms: Photobiomodulation therapy, Monte Carlo simulation, spinal cord injury, dosimetry.

1. Introduction

Millions of people are affected by spinal cord injuries (SCIs) each year, sometimes in life-changing ways. Although animal models have been used to evaluate a variety of experimental treatment strategies to address SCIs, fully restorative treatments for SCIs have not yet emerged [1], [2].

Several studies have demonstrated that photobiomodulation therapy (PBMT) may encourage wound healing, reduce inflammation, lessen pain levels, and promote peripheral nerve generation [3]. Many studies have shown that PBMT has the capacity to repair nerves and enhance spinal cord functionality in animal models (see Table 1) [4]–[11]. These researchers assess the effectiveness of PBMT using the fluence (“dose”) on the skin surface as the chief dose assessment index without considering the irradiation parameters or the physiological parameters of the animal’s weight. Piao et al. [12] recently demonstrated that the fluence rate, which reaches the targeted

TABLE 1
Summary of the Applied Irradiation Parameters for PBMT Contusion SCI Rat Model Studies [4]–[11]

Study	Age/weight	Wavelength (nm)	Power (mW)	Beam area (cm^2)	Irradiation time (s/day)	Fluence on surface (J/cm^2)	Treatment period (days)
Rochkind et al. [4]	13 weeks	780 CW laser	250	-	1800	-	14
Byrnes et al. [5]	200–300 g	810 CW laser	150	0.3	2,997	1,589	14
Wu et al. [6]	200–300 g	810 CW laser	150	0.3	2,997	1,589	14
Paula et al. [7]	300–350 g	780 CW laser	44	0.196	28	6.16	21
Sotoudeh et al. [8]	400–450 g	810 CW laser	150	0.3	4,800	1,589	3
Hu et al. [9]	7 weeks	675 CW LED	26.25	75	1,800	63	7
Veronez et al. [10]	10 weeks	808 CW laser	30	0.028	141; 212; 282	151; 227; 302	7
Song et al. [11]	220–260 g	810 CW laser	150	0.3	3,000	1,500	14

SCI area, depends on the tissue thickness at the injury site and the position of the probe relative to the injury site, that is, applying a certain level of fluence on the skin does not mean that the injury site will receive the same fluence rate. Piao el al. [12] also showed that on-contact surface irradiation increased the transmitted light by 67% compared with off-contact surface irradiation. Conversely, Krishna et al. [13] monitored the rat weight in SCI contusion models, finding notable fluctuations in weight over the 14-day study; the weight increased within the first few days of the SCI as a result of water retention and then fell by 10–12% in the following 10 days. Rat weight fluctuations may affect the tissue thickness over the injury site, which could cause unknown fluctuations in the fluence delivered to the injury site during PBMT; this could mean that it is not possible to compare research solely based on the fluence values stated in studies. Furthermore, animal SCI PBMT studies have employed many different rat sizes (weight/age), ranging from 200 to 450 g (as shown in Table 1), which increases the complexity of comparing these studies.

Another consideration is that PBMT has been shown to have a biphasic dose-response pattern [14]. A small dose may trigger no response from irradiated tissue, while extremely high doses could result in inhibition. This means that the selection of PBMT parameters over the course of the experiment is crucial for accuracy. Researchers could be unintentionally providing doses that are higher or lower than what they expect. If the precise level of fluence received by the injury site is unknown, then the results could be significantly affected, which creates significant difficulties for other researchers who attempt to reproduce the research. Moreover, the credibility of PBMT in the medical field could be substantially affected.

Recently, a Monte Carlo (MC) simulation, a fundamental and flexible approach used to model light propagation in tissues, was employed with a 3D SCI rat model to understand the influence of the irradiation parameters on the fluence delivered to the injury site [15]. In this study, we employed an MC simulation to investigate the influence of rat body weight fluctuations and different irradiation parameters on the fluence delivered to the injury site during treatment.

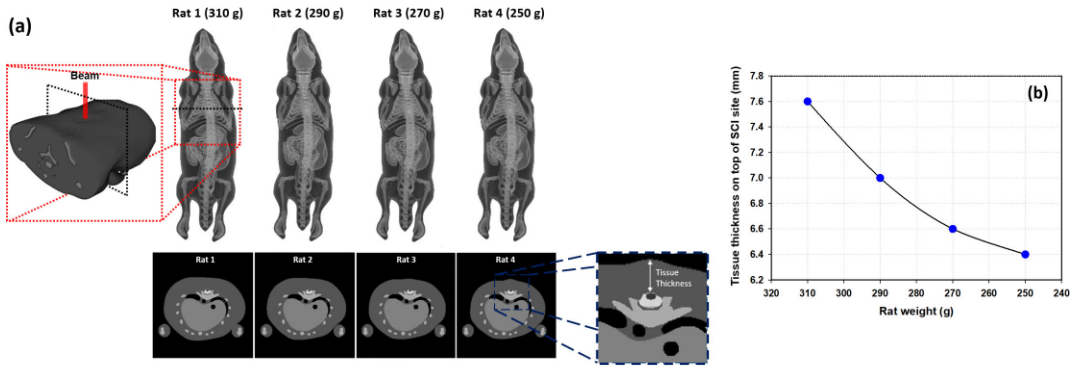

Fig. 1. (a) 3D visualization of four SCI rat models: Rat 1 (310 g), Rat 2 (290 g), Rat 3 (270 g), and Rat 4 (250 g). The dotted red box is the 3D model region used in the MC simulation and shows the position of the beam. The dotted black line shows the cross-section of the SCI rat model at the center of the hematoma. The rat models were modified by removing the T10 spinous process and embedding an ellipsoid-shaped hematoma with a volume of $0.2 \times 0.2 \times 0.2$ mm^3 in the spinal cord. The dashed blue box shows a more detailed cross-section of the SCI rat model. (b) The thickness of the tissue on top of the SCI site as a function of the rat weight.

2. Experimental Details

2.1. Spinal Cord Injury Rat Model

In this study, we used a 3D SCI phantom rat model that was described in detail in a previously published paper [16]. Four phantom rat models were constructed, all of which were the same age (11 weeks) but had different weights (Rat 1 = 310 g, Rat 2 = 290 g, Rat 3 = 270 g, and Rat 4 = 250 g) [17] (Fig. 1). In the model, various indices were used to refer to the type of biological tissue at the injury site to assign their optical properties in the MC simulation.

2.2. Monte Carlo Simulation

Light propagation was simulated in four phantom rat models using Monte Carlo eXtreme (MCX), which was developed by Fang and Boas [18]. Table 2 shows the optical properties of the SCI rat tissue, including the skin, muscle, bone, soft tissue, spinal cord, and blood ($SpO_2 > 98\%$), at three different wavelengths according to the reference data reported in previous studies [19]–[22]. In this study, a total of 360 irradiation parameters were simulated: four rat models with different weights (Rat 1 = 310 g, Rat 2 = 290 g, Rat 3 = 270 g, and Rat 4 = 250 g), three wavelengths (660, 810, and 980 nm), two beam types (Gaussian and top-hat), and 15 beam diameters (0.02, 0.04, 0.1, 0.2, 0.4, 0.8, 1.6, 2.0, 4.0, 6.0, 8.0, 12, 16, 20, and 24 mm). For all the simulated beams, the fluence on the surface was fixed (25 J/cm^2). For each simulation, 10^8 photons were launched, which took approximately 30 seconds to complete on three Nvidia GTX 1080 Ti graphic processing units (GPU).

For each simulation, the fluence rate profiles were calculated using MCX. To understand the effect of the PBMT irradiation parameters on the different generated SCI rat models by weight, the fluence distributions were further analyzed. The total accumulated fluence (AF) within the SCI site is the total fluence value along all voxels belonging to the injury site. The percentage differences of the AF (%ΔAF) within the SCI site between the heaviest rat (Rat 1) and the three other rat models (Rat 2, Rat 3, and Rat 4) were computed using the following equation:

$$\%\Delta AF_{i-1} = \frac{AF_i - AF_1}{AF_1} \times 100\% \quad (1)$$

where AF_i is the accumulated fluence for Rat i (i = 2, 3, or 4), and AF_1 is the accumulated fluence at the injury site for Rat 1. The results were plotted only for the Gaussian beam for different diameters

TABLE 2

Optical Properties of SCI Rat Tissue With 660, 810, and 980 nm Wavelengths [19]–[22]. The Refractive Indices (n) for All Tissues Were Assumed to be 1.37. The Unit Used for Absorption (μa), Scattering Coefficient (μs), and Reduced Scattering Coefficient (μ's) is mm^{-1}

Tissue type	660 nm				810 nm				980 nm			
	μ_a	μ_s	g	μ'_s	μ_a	μ_s	g	μ'_s	μ_a	μ_s	g	μ'_s
Skin	0.0340	25.80	0.900	2.580	0.0195	19.20	0.900	1.920	0.045	14.0	0.900	1.400
Muscle	0.0870	8.61	0.900	0.861	0.0270	6.87	0.900	0.687	0.051	5.56	0.900	0.556
Soft Tissue	0.0890	13.23	0.900	1.323	0.0212	10.16	0.900	1.016	0.1640	7.955	0.900	0.796
Bone	0.0100	15.23	0.900	1.523	0.0070	13.28	0.900	1.328	0.0210	11.93	0.900	1.193
Spinal Cord	0.0216	15.47	0.900	1.547	0.0134	11.13	0.900	1.113	0.0405	8.184	0.900	0.818
Blood (SpO2 > 98%)	0.1500	87.61	0.983	1.489	0.4000	76.10	0.983	1.294	0.6800	62.68	0.9798	1.266

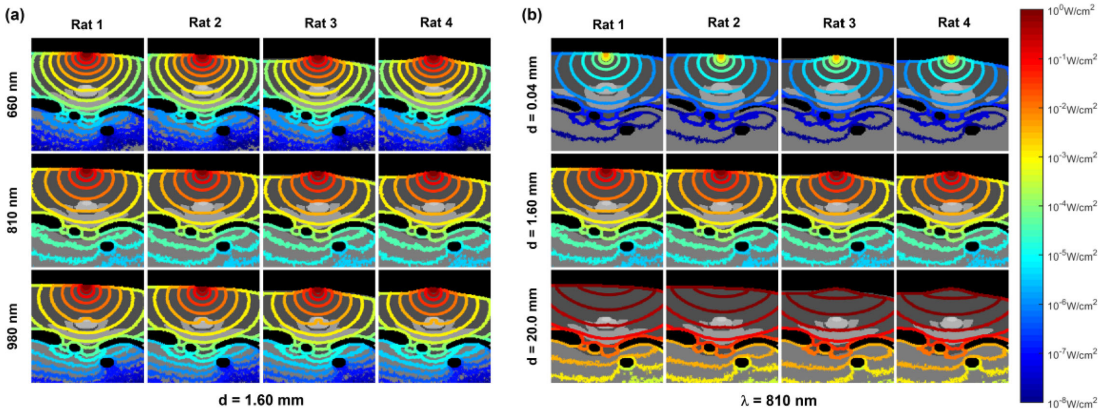

Fig. 2. Photobiomodulation iso-F contour in SCI rat models for Gaussian beams with (a) different wavelengths (660, 810, and 980 nm) and different rat weights (Rat 1 = 310 g, Rat 2 = 290 g, Rat 3 = 270 g, and Rat 4 = 250 g) for a beam diameter of 1.60 mm; and (b) different diameters (0.04, 1.60, and 20.0 mm) and different rat weights (Rat 1 = 310 g, Rat 2 = 290 g, Rat 3 = 270 g, and Rat 4 = 250 g) for a beam wavelength of 810 nm. The notation d represents the diameter. The iso-F contour shown here is 10^0–10^{-8} W/cm^2.

(1.6, 6, and 20 mm) and different wavelengths (660, 810, and 980 nm). The top-hat beam data are not shown due to their similarity.

3. Results

Fig. 2a illustrates the influence of a variety of wavelengths and rat weights on the fluence received by the SCI site. The iso-fluence (iso-F) contour is illustrated for 10^0–10^{-8} W/cm^2. The 810 nm beam had a greater depth of penetration than either the 660 nm or the 980 nm beam. The 810 nm beam, with an iso-F contour of 10^{-2} W/cm^2, reached and penetrated the SCI site; the 980 nm beam, with identical specifications, only reached the surface of the site; and the 660 nm beam, with an iso-F contour of 10^{-3} W/cm^2, did not reach the site. Additionally, decreasing the rat weight increased

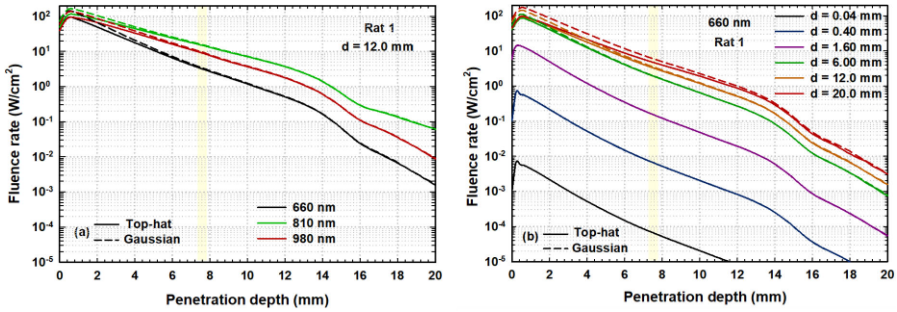

Fig. 3. Fluence rate as a function of the penetration depth for (a) different beam wavelengths and beam types and (b) different beam diameters and beam types. The yellow-shaded region denotes the injury site depth. The notation d represents the diameter. The model of Rat 1 (310 g) is shown in the figure.

the penetration depth at the injury site. The fluence distributions in the rat model for a variety of weights and beam diameters are illustrated in Fig. 2b. The iso-F contour that reached the injury site for the 20.0 mm beam diameter (10^0 W/cm^2) was significantly higher than that of the smaller beam diameter (0.04 mm; 10^{-5} W/cm^2). This is because the fluence on the surface was fixed, resulting in higher beam power as the beam diameter increased. As the beam broadened, a central region of uniform fluence rate developed in the center of the beam. This development means that accurate positioning is more important for narrower beams than for larger beams. As previously mentioned, when the rat weight decreased, the tissue thickness on top of the injury site decreased (as shown in Fig. 1b), and a greater fluence reached the injury site. On a different note, the beam type had an insignificant effect on the iso-F distribution that reached the injury site (data not shown).

Fig. 3 illustrates the fluence as a function of the penetration depth for the previously mentioned irradiation parameters. Only the heaviest rat (Rat 1) is shown. Fig. 3a demonstrates that for identical types of beams that reached the upper surface of the injury site, the 810 nm wavelength had the greatest fluence of 16.2 W/cm^2, while that of the 980 nm wavelength was 9.52 W/cm^2 and the 660 nm wavelength was only 3.42 W/cm^2. Separating the fluence that reached certain penetration depths was difficult when using an identical beam size but a different beam type; that is, the beam type had less influence than the wavelength. Fig. 3b shows the penetration fluence attenuation for three different beam diameters for each beam type. As the beam size increased, the light penetration depth increased significantly. Using a top-hat beam that reached the upper surface of the injury site, which has the smallest diameter d $=$ 0.04 mm, a fluence rate of 7.34 $\times$ 10^{-5} W/cm^2 was obtained. For d $=$ 12.00 mm, a fluence of 3.53 W/cm^2 was obtained, and for d $=$ 20.0 mm, a fluence of 4.91 W/cm^2 was obtained. For large beams, the influence of the beam type was easy to discern at a shallow penetration depth, providing an illustration of how increasing or decreasing the tissue thickness above the injury site can impact the AF.

Fig. 4 illustrates the AF for a rat model when the beam type is a function of the beam diameter at various wavelengths (660, 810, and 980 nm). The figure shows that increasing the beam diameter for fixed fluence on the surface significantly increased the AF. Furthermore, a variety of AFs occurred with fluctuating rat weights due to the reduced tissue thickness at the injury site. Beams with an 810 nm wavelength had AFs that were approximately four times and two times higher than those with a 660 nm wavelength and a 980 nm wavelength, respectively. In terms of beam type, Gaussian beams had a larger AF than top-hat beams; this effect was more pronounced with a larger beam. Therefore, researchers should consider the differences in the transmission of light for different wavelengths and rat weights. Significantly, therapeutic efficacy cannot be assessed by simply matching the AF due to a lack of understanding about the PBMT mechanism.

Fig. 5 shows the $\triangle$AF between the heaviest rat (Rat 1) and the remaining three rats, which was calculated using Equation (1), for three beam diameters (1.6, 6, and 20 mm) and different wavelengths. As the weight of the rat changed (Rat 1 to Rat 4), the $\triangle$AF was higher for the 660

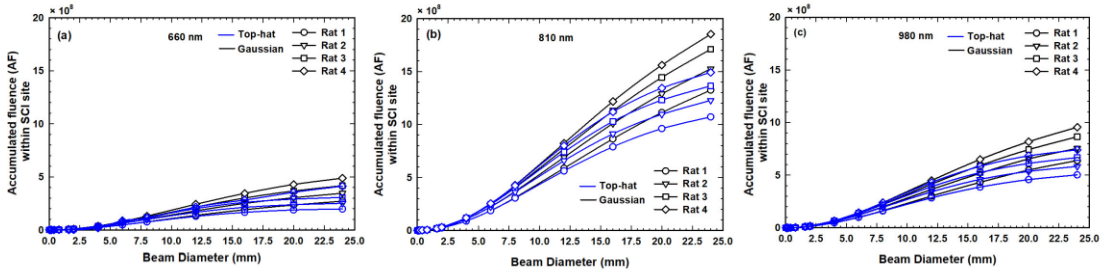

Fig. 4. The accumulated fluence (AF) within the SCI site as a function of the beam diameter for different rat weights and different beam types: (a) 660 nm, (b) 810 nm, and (c) 980 nm.

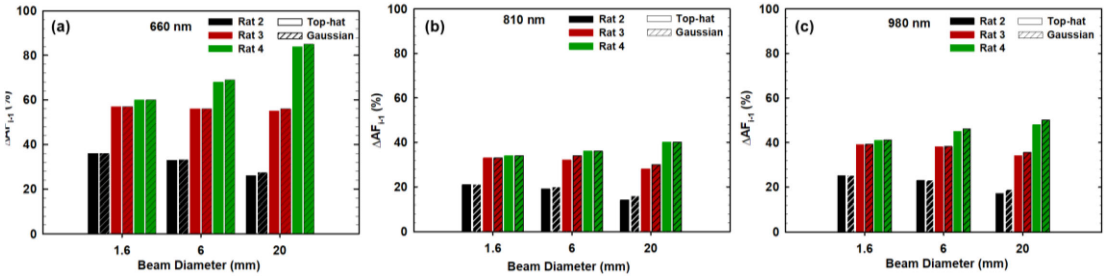

Fig. 5. The percentage change in the accumulated fluence within the SCI site (ΔAF_{i-1}) between Rat 1 (310 g) and Rats 2–4 (290–250 g) for different beam diameters (1.6, 6, and 20 mm) and different wavelengths: (a) 660 nm, (b) 810 nm, and (c) 980 nm.

nm beam ($\Delta AF_{1\text{-}4} \approx 85\%$) than for the 980 nm ($\Delta AF_{1\text{-}4} \approx 50\%$) and 810 nm ($\Delta AF_{1\text{-}4} \approx 40\%$) beams. For a specific wavelength, the ΔAF of the Gaussian beam was slightly higher than that of the top-hat beam. Overall, the large Gaussian beam with the 660 nm wavelength had the highest ΔAF when compared with other beam parameter combinations. Therefore, when calculating the fluence that needs to be delivered to the injury site, researchers should consider the rat weight more when using a 660 nm wavelength, due to tissue thickness strong effect on light propagation, than when using an 810 wavelength or a 980 nm wavelength.

4. Discussion

To the best of our knowledge, the present work is the first MC-simulated study on the effect of the subject's weight on PBMT dosimetry. Researchers typically use three parameters to control the light source: beam area, irradiation time, and power. In combination, these parameters can be adjusted to control the irradiance and fluence of the treatment that is administered [23], [24]. Nevertheless, every patient is different; patients have different skin colors and thicknesses, body types, and responses to treatment [24]. Dosimetry depends on much more than just the irradiation parameters; it also depends on the specific characteristics of the patient, the physiological tissue conditions, and the proximity of the beam relative to the injury site [23], [24]. While calculating the fluence amount that needs to be delivered to the patient is relatively easy, determining the fluence amount that is delivered to the injury site is less straightforward. To achieve optimal PBMT, a sufficient fluence must be delivered to the injury site with a suitable wavelength, irradiance, irradiation time, and treatment period to accomplish the required clinical response [23], [24]. Furthermore, PBMT has been well-recognized to present a biphasic dose response [24]. Applying a lower fluence than the minimum threshold may not trigger responses, whereas a higher fluence

than the maximum threshold may cause inhibition [24]. Therefore, understanding the physics of laser-tissue interactions is as important as understanding their biochemistry and physiology.

In this study, we found that SCI researchers unintentionally delivered different fluences (doses) for each treatment session; thus, a biphasic dose response might affect the outcomes of their studies. All these interrelated parameters and patient-specific conditions have made PBMT dosimetry a pitfall for several research studies and clinical approaches. One way to reduce the uncertainty in the fluence delivered to the injury site for each patient is by using an MC simulation.

5. Conclusion

This study performed MC simulations using four computer-simulated rat models. All rats were aged 11 weeks but each rat had a different weight. Various irradiation parameters were employed to assess the impact of these factors on the fluence delivery at the SCI site. The results showed that 810 nm was a more ideal wavelength than others for SCI PBMT treatment due to the low absorption coefficient of SCI rat tissue at 810 nm, which results in deeper light penetration. Furthermore, as the rat weight decreased, the tissue thickness on top of the SCI decreased; therefore, the AF increased for all wavelengths. However, the $\triangle$AF noticeably differed between wavelengths when the rat weight changed, which was attributable to the optical properties of the tissue. As the rat weight changed (310 g to 250 g), the $\triangle$AF for the 660 nm beam increased significantly ($\triangle AF_{1\text{-}4} \approx 85\%$) compared with the 980 nm beam ($\triangle AF_{1\text{-}4} \approx 50\%$) and the 810 nm ($\triangle AF_{1\text{-}4} \approx 40\%$) beam. This increase caused an increase in the complexity involved in knowing the fluence that is delivered to the SCI site and the reproducibility of the study. Overall, when using a large Gaussian beam with a 660 nm wavelength for an SCI rat model (or when the animal or patient's weight changes during the treatment duration), researchers should consider the weight more than when using other wavelengths (such as 810 or 980 nm) to ensure that the applied fluence is within the optimal range and that the PBMT biphasic dose response does not influence the outcome of the study. To optimize PBMT and apply the optimal dose, researchers must account for weight before and during the experiment.

Acknowledgements

The authors would like to thank the anonymous reviewers for their valuable suggestions.

References

[1] A. J. Kastin and W. Pan, "Targeting neurite growth inhibitors to induce CNS regeneration," *Curr. Pharmaceut. Des.*, vol. 11, no. 10, pp. 1247–1253, 2005.
[2] B. Atalay *et al.*, "Antibodies neutralizing Nogo-A increase pan-cadherin expression and motor recovery following spinal cord injury in rats," *Spinal Cord*, vol. 45, no. 12, pp. 780–786, 2007.
[3] M. R. Hamblin, "Shining light on the head: Photobiomodulation for brain disorders," *BBA Clin.*, vol. 6, pp. 113–124, 2016.
[4] S. Rochkind, A. Shahar, M. Amon, and Z. Nevo, "Transplantation of embryonal spinal cord nerve cells cultured on biodegradable microcarriers followed by low power laser irradiation for the treatment of traumatic paraplegia in rats," *Neurological Res.*, vol. 24, no. 4, pp. 355–360, 2002.
[5] K. R. Byrnes *et al.*, "Light promotes regeneration and functional recovery and alters the immune response after spinal cord injury," *Lasers Surg. Med.*, vol. 36, no. 3, pp. 171–185, 2005.
[6] X. Wu *et al.*, "810 nm Wavelength light: An effective therapy for transected or contused rat spinal cord," *Lasers Surg. Med.*, vol. 41, no. 1, pp. 36–41, 2009.
[7] A. A. Paula, R. A. Nicolau, O. Lima Mde, M. A. Salgado, and J. C. Cogo, "Low-intensity laser therapy effect on the recovery of traumatic spinal cord injury," *Lasers Med. Sci.*, vol. 29, no. 6, pp. 1849–1859, 2014.
[8] A. Sotoudeh, A. Jahanshahi, S. Zareiy, M. Darvishi, N. Roodbari, and A. Bazzazan, "The influence of low-level laser irradiation on spinal cord injuries following ischemia-reperfusion in rats," *Acta Cirurgica Brasileira*, vol. 30, no. 9, pp. 611–616, 2015.
[9] D. Hu, S. Zhu, and J. R. Potas, "Red LED photobiomodulation reduces pain hypersensitivity and improves sensorimotor function following mild T10 hemicontusion spinal cord injury," *J. Neuroinflam.*, vol. 13, no. 1, p. 200, 2016.
[10] S. Veronez *et al.*, "Effects of different fluences of low-level laser therapy in an experimental model of spinal cord injury in rats," *Lasers Med. Sci.*, vol. 32, no. 2, pp. 343–349, 2017.

[11] J. W. Song *et al.*, "Low-level laser facilitates alternatively activated macrophage/microglia polarization and promotes functional recovery after crush spinal cord injury in rats," *Sci. Rep.*, vol. 7, no. 1, p. 620, 2017.
[12] D. Piao, L. A. Sypniewski, C. Bailey, D. Dugat, D. J. Burba, and L. De Taboada, "Flexible nine-channel photodetector probe facilitated intraspinal multisite transcutaneous photobiomodulation therapy dosimetry in cadaver dogs," *J. Biomed. Opt.*, vol. 23, no. 1, pp. 1–4, 2018.
[13] V. Krishna *et al.*, "A contusion model of severe spinal cord injury in rats," *J. Visualized Experiments*, no. 78, 2013, Art. no. 50111.
[14] Y. Y. Huang, S. K. Sharma, J. Carroll, and M. R. Hamblin, "Biphasic dose response in low level light therapy – An update," *Dose Response*, vol. 9, no. 4, pp. 602–618, 2011.
[15] A. Shuaib and A. K. Bourisly, "Photobiomodulation optimization for spinal cord injury rat phantom model," *Transl. Neurosci.*, vol. 9, pp. 67–71, 2018.
[16] W. P. Segars, B. M. Tsui, E. C. Frey, G. A. Johnson, and S. S. Berr, "Development of a 4-D digital mouse phantom for molecular imaging research," *Mol. Imag. Biol.*, vol. 6, no. 3, pp. 149–159, 2004.
[17] T. Xie and H. Zaidi, "Age-dependent small-animal internal radiation dosimetry," *Mol. Imag.*, vol. 12, no. 6, pp. 364–375, 2013.
[18] Q. Fang and D. A. Boas, "Monte carlo simulation of photon migration in 3D turbid media accelerated by graphics processing units," *Opt. Express*, vol. 17, no. 22, pp. 20178–20190, 2009.
[19] S. L. Jacques, "Optical properties of biological tissues: A review," *Phys. Med. Biol.*, vol. 58, no. 11, pp. R37–R61, 2013.
[20] N. Bosschaart, G. J. Edelman, M. C. Aalders, T. G. van Leeuwen, and D. J. Faber, "A literature review and novel theoretical approach on the optical properties of whole blood," *Lasers Med. Sci.*, vol. 29, no. 2, pp. 453–479, 2014.
[21] A. N. Bashkatov, E. A. Genina, and V. V. Tuchin, "Optical properties of skin, subcutaneous, and muscle tissues: A review," *J. Innov. Opt. Health Sci.*, vol. 4, no. 01, pp. 9–38, 2011.
[22] A. Pifferi *et al.*, "Optical biopsy of bone tissue: A step toward the diagnosis of bone pathologies," *J. Biomed. Opt.*, vol. 9, no. 3, pp. 474–480, 2004.
[23] M. A. Hadis *et al.*, "The dark art of light measurement: Accurate radiometry for low-level light therapy," *Lasers Med. Sci.*, vol. 31, no. 4, pp. 789–809, 2016.
[24] R. Zein, W. Selting, and M. R. Hamblin, "Review of light parameters and photobiomodulation efficacy: Dive into complexity," *J. Biomed. Opt.*, vol. 23, no. 12, pp. 1–17, 2018.